

# Absolute dating of the European Neolithic using the 5259 BC rapid $^{14}\text{C}$ excursion

Received: 7 October 2023

Accepted: 30 April 2024

Published online: 20 May 2024

 Check for updates

Andrej Maczkowski<sup>1,2</sup>✉, Charlotte Pearson<sup>3</sup>, John Francuz<sup>1</sup>,  
Tryfon Giagkoulis<sup>4</sup>, Sönke Szidat<sup>2,5</sup>, Lukas Wacker<sup>6</sup>,  
Matthias Bolliger<sup>1,2,7</sup>, Kostas Kotsakis<sup>4</sup> & Albert Hafner<sup>1,2</sup>

Abrupt radiocarbon ( $^{14}\text{C}$ ) excursions, or Miyake events, in sequences of radiocarbon measurements from calendar-dated tree-rings provide opportunities to assign absolute calendar dates to undated wood samples from contexts across history and prehistory. Here, we report a tree-ring and  $^{14}\text{C}$ -dating study of the Neolithic site of Dispilio, Northern Greece, a waterlogged archaeological site on Lake Kastoria. Findings secure an absolute, calendar-dated time using the 5259 BC Miyake event, with the final ring of the 303-year-long juniper tree-ring chronology dating to 5140 BC. While other sites have been absolutely dated to a calendar year through  $^{14}\text{C}$ -signature Miyake events, Dispilio is the first European Neolithic site of these and it provides a fixed, calendar-year anchor point for regional chronologies of the Neolithic.

The Neolithic period in western Eurasia marks one of the most important transitions in human social, economic, and technological history. This transition, which lasted several millennia, is chiefly characterised by the appearance and gradual adoption of agriculture and animal husbandry accompanied by increasing social and material culture complexity. The appearance of the first Neolithic communities on the Aegean coasts and in Northern Greece, and hence in continental Europe, is dated to around 6500 BC<sup>1–6</sup>. The expansion of the Neolithic settlements further inland to the North was a rapid process<sup>7</sup>. Consequently, their precise dating is essential to our understanding of neolithisation processes in Europe and critical to assessments of the environmental footprint of the new farming subsistence practices. However, the temporal resolution of archaeological and environmental proxies in the region is highly variable, producing significant discrepancies between various chronological and terminological systems that deal with the periodisation of the Neolithic<sup>8</sup>. The combination of tree-ring dating (dendrochronology) and rapid  $^{14}\text{C}$  excursions has been previously used for the absolute dating of sites only from the Common Era<sup>9–12</sup>. Here, we present the absolute dating of the 6th millennium BC lake-dwelling site of Dispilio in Northwestern Greece. Our

results may provide the basis for absolute dendrochronological dating of other Neolithic sites in the region (Fig. 1).

Tree-rings enable high-resolution dating, the possibility of annually resolved climatic reconstruction, and multidisciplinary chronological synchronization, often to a single growth season of a specific calendar year<sup>13</sup>. Until recently<sup>9</sup>, dendrochronological dating was possible only against reference tree-ring chronologies, which are continuous, unbroken sequences of tree-ring width records extending from the present back to the distant past. Based on known dates from living trees, calendar-years are assigned to tree-rings and then extended into the past using climatically constrained, region-specific, continuous tree-ring growth patterns. Long-term concentrated efforts in search for old wood samples have resulted in the construction of long tree-ring records extending back many thousands of years; these are widely applied to dating<sup>14–16</sup> and paleoclimatic analyses<sup>17,18</sup>, shedding light on past human and environmental interactions. However, these records are geographically limited and rare. Moreover, many prehistoric tree-ring chronologies are only approximately constrained on a calendar timescale through conventional  $^{14}\text{C}$  wiggle-matching and have no absolute calendar anchor.

<sup>1</sup>Institute of Archaeological Sciences, University of Bern, Bern, Switzerland. <sup>2</sup>Oeschger Centre for Climate Change Research, University of Bern, Bern, Switzerland. <sup>3</sup>Laboratory of Tree-Ring Research, University of Arizona, Tucson, USA. <sup>4</sup>School of History and Archaeology, University of Thessaloniki, Thessaloniki, Greece. <sup>5</sup>Department of Chemistry, Biochemistry and Pharmaceutical Sciences, University of Bern, Bern, Switzerland. <sup>6</sup>Laboratory for Ion Beam Physics, ETH Zürich, Switzerland. <sup>7</sup>Laboratory for Dendrochronology, Archaeological Service of Canton of Bern, Bern, Switzerland.

✉ e-mail: [andrej.maczkowski@unibe.ch](mailto:andrej.maczkowski@unibe.ch)

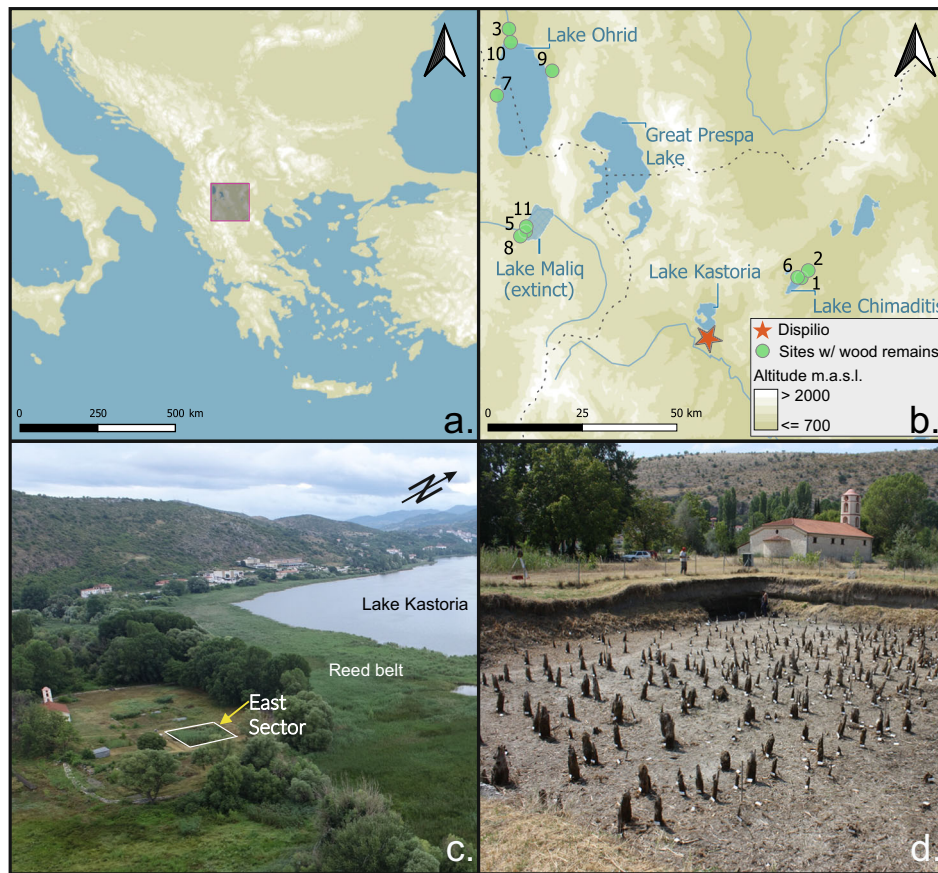


**Fig. 1 | Location of the archaeological site of Dispilio and detailed view of the trench analysed.** **a** map of S-E Europe highlighting the location of the enlarged area in **b**. **b** Location of Dispilio, and of other Neolithic sites within 100 km with reported good wood preservation and similar chronological placement, thus holding significant potential for dendrochronological cross-dating with Dispilio. Sites depicted: 1-Anarghiri III; 2-Anarghiri IXb; 3-Crkveni Livadi; star-Dispilio; 5-Dunavec; 6-Limnochori II; 7-Lin 3; 8-Maliq; 9-Ohridati/Penelopa; 10-Ustie na Drim,

11-Sovjan; maps produced in QGIS 3.16, EPSG 32634, with SRTM<sup>112</sup> elevation data; Lake Maliq according to Fouache et al.<sup>113</sup>. **c** drone photograph of the site of Dispilio and its surroundings, the dendrochronologically analysed East Sector marked in the foreground. **d** close-up of the East Sector before sampling of wooden elements in 2019, vertical elements are seen projecting from the ground, each marked with a white label. (**a**, **b** A. Maczkowski; **c** M. Hostettler; **d** Dispilio Excavation Archive).

This limitation can now be overcome by a new hybrid form of dendrochronological and single-year radiocarbon analyses. Annual measurements of  $^{14}\text{C}$  in dendrochronologically dated Holocene tree-rings have revealed the occurrence of rapid short-term spikes in atmospheric  $^{14}\text{C}$  concentration in the past<sup>19,20</sup>. These  $^{14}\text{C}$  spikes, also called Miyake or solar energetic particle (SEP) events, are uniquely suitable for absolute dating of any wooden objects with detectable annual rings<sup>9,21</sup>. The discovery of these short-term events has also led to a proliferation of annual  $^{14}\text{C}$  measurements on single tree-rings, now spanning several millennia<sup>22–24</sup>. The mechanisms behind these  $^{14}\text{C}$  events are still debated<sup>25,26</sup>. However, a broadly accepted explanation is that they result from coronal mass ejections from the Sun<sup>25,27–29</sup>. These lead to a surge of SEPs colliding with the Earth's atmosphere, which increases the production of cosmogenic radionuclides<sup>22,29</sup>. To date, only five events<sup>19,20,22,30</sup> involving an atmospheric  $^{14}\text{C}$  increase of  $\geq 1\%$  within 2 years<sup>22</sup> have been confirmed. Of these, the two most recently discovered events are in the first half of the Holocene, in 7176 BC and 5259 BC<sup>22</sup>, offering now the possibility for absolute annual dating of wood from the 8th and 6th millennia BC using annual  $^{14}\text{C}$  measurements.

In temperate climates, wood and other organic materials can be preserved only in very stable conditions, as in low-oxygen waterlogged sediments at wetland archaeological sites<sup>31–33</sup>. Excavated wetland sites are very numerous and often excavated in Central

Europe, and several wetland sites have also been found and excavated in south-eastern Europe, notably in the south-western Balkans<sup>34–40</sup>. Dendrochronological work on these sites has led to the construction of several tree-ring width chronologies, which were approximately fixed in time by  $^{14}\text{C}$  wiggle matching<sup>41,42</sup>. Dispilio on the shores of Lake Kastoria in north-western Greece is an archaeologically significant prehistoric wetland site in the region, considering that it is the only “pile-dwelling” settlement in the Balkans to be systematically excavated over multiple years and over a large area. Numerous lines of evidence have yielded detailed results on the site's geoarchaeology<sup>39</sup>, palynology<sup>43,44</sup>, anthracology<sup>45,46</sup>, wood-working technology<sup>47</sup>, and material culture<sup>48,49</sup> (Fig. 2). The approximate calendar-age chronology of the site has been established through radiocarbon dates, mostly performed on charcoal samples<sup>39,50</sup>. Charcoal is susceptible to the so-called “inbuilt age”, which may produce overly old radiocarbon dates. The calibrated date-ranges point to settlement phases between the later Middle Neolithic ( $\sim 5600$  cal BC<sup>51</sup>) and the Bronze Age ( $\sim 2100$  cal BC<sup>50</sup>). The excavations at Dispilio have also yielded a great number of wooden remains, with over 1200 mapped construction elements in the site's East Sector to date (Fig. 1c). Yet despite the extensive remains of wooden construction elements, no systematic sampling and no dendrochronological studies have yet been conducted at the site. The value of developing a precise and accurate calendar-dated



**Fig. 2 | Archaeological finds from Neolithic Dispilio. a** almost completely preserved ornate anthropomorphic vessel from Late Neolithic. Many similar ones have been recovered from the site, scale in cm. **b** bone spear or harpoon tip with

preserved hafting adhesives, scale in cm. **c** an assemblage of Late Neolithic personal adornments (a–c, Dispilio Excavation Archive).

chronological sequence using these wooden remains is further enhanced by the fact that the site of Dispilio has yielded more than 1700 complete and fully reconstructed ceramic vessels: one of the largest complete Neolithic ceramic assemblages in Europe. Tree-ring dating at Dispilio can therefore be used in conjunction with the ceramics typology network to underpin and improve the relative chronology of the entire region.

In 2019 a large-scale fieldwork campaign took place at Dispilio's Eastern Sector (Fig. 1d). Over 900 piles were mapped, of which 787 were sampled for the first dendrochronological analysis. The results provided a 'floating' oak tree-ring chronology spanning 120 years and an overlapping juniper tree-ring chronology spanning 303 years. However, this dendrochronological record could not be dated absolutely because despite the existence of several millennia-long tree-ring chronologies in the Eastern Mediterranean<sup>17,52,53</sup>, none extend back to 7500 years. Here, we overcome this limitation by using the combination of dendrochronological and single-year radiocarbon analysis (Fig. 3), placing the last ring of the Dispilio juniper chronology at 5140 BC. To our knowledge, no calendar-year absolute dating has been achieved yet for any other Neolithic site in the wider Mediterranean region.

## Results

### Dendrochronology

Wood samples from Dispilio were first sorted by genus, then measured and cross-dated into tree-ring width (TRW) chronologies. Then, individual tree-rings from the cross-dated wood samples were sampled for <sup>14</sup>C measurements to identify the 5259 BC <sup>14</sup>C spike in the juniper tree-ring chronology, which provides the absolute calendar-year placement of the tree-ring chronology. Of the total wood samples from the 2019 fieldwork ( $n = 787$ ), 23% were cross-dated into two master tree-ring width (TRW) chronologies. Wood anatomical species determination revealed that the majority of the wooden piles came from juniper (*Juniperus* spp., 62%) and oak (*Quercus* spp., 21%) wood. The third most abundant genus was pine (*Pinus* spp., 17%), which was not suitable for dendrochronological cross-dating given the low number of annual rings on most pine samples. Due to the wood-anatomical intra-genus similarity of junipers<sup>54,55</sup>, and of deciduous oaks from the subgenus *Quercus*<sup>56</sup>, a definitive species-level identification was not possible. Based on the distribution of modern tree species in the region<sup>45,57,58</sup>, Dispilio oak wood samples most likely come from *Quercus frainetto*, *Q. petraea*, and/or *Q. pubescens* wood, and the junipers are most likely *Juniperus excelsa*, *J. foetidissima*, and/or *J. deltoides* (cf. *J. oxycedrus*).

The oak TRW chronology extends over 120 years and is composed of 58 wood samples (Fig. 4). It consists of tree-ring sequences with an average segment length of 66 years. Some sapwood was present on most of the oak samples ( $n = 45$ ); however, the final growth ring or "waney-edge", which is important for archaeological interpretation, was conserved on only four pieces, as a result of either the lower

durability of oak sapwood or its intentional removal. The mean inter-series correlation<sup>59</sup> of the oak tree-ring sequences is 0.51.

A 303-years-long juniper TRW-chronology was also constructed with 118 tree-ring sequences and an average segment length of 86 years (Fig. 4). The mean inter-series correlation<sup>59</sup> of the juniper chronology is 0.62. Juniper wood's chemical<sup>60</sup> and physical<sup>61</sup> properties give it high resistance to degradation. These qualities made juniper wood the material of choice for construction purposes in many ancient societies in the Eastern Mediterranean<sup>62–64</sup>. The preservation of juniper wood in Dispilio is also exceptional and the waney edge on junipers is quite common, enabling an annually resolved reconstruction of the building phases and occupation duration on the site (Fig. 4b).

All samples with a preserved waney edge had a final growth ring terminating with latewood, thus implying a felling date during the dormant period of the trees between late summer/autumn and early spring. The juniper and oak TRW chronologies have robust dendrochronological dating against each other ( $t$ -value = 4.9<sup>65</sup> and =5.1<sup>66</sup>; GLK = 63%<sup>67</sup>) over a period of 108 years where sample replication is >4. This dendrochronological cross-dating between the two chronologies, considering that the oak chronology does not span the Miyake event, is independently supported by a conventional <sup>14</sup>C wiggle-matching model of 11 <sup>14</sup>C measurements performed on tree-rings comprising the oak TRW chronology<sup>51</sup> (Supplementary Note 1).

### Tree-ring <sup>14</sup>C cosmogenic signature and calendar-year dating

The preliminary modelled end-date range for the juniper tree-ring width chronology was established through a conventional radiocarbon wiggle-matching model<sup>68,69</sup>, with the IntCal20<sup>70</sup> radiocarbon calibration curve (see Supplementary Note 1). On the basis of this coarse resolution wiggle-match dating we identified the wood samples and their corresponding tree-rings that should approximately span the period of the 5259 BC Miyake event. Four individual juniper wood samples were selected for annual <sup>14</sup>C measurements, and the tree-rings approximately spanning the predicted position of the 5259 BC Miyake event were dissected at annual resolution (Fig. 3a and Supplementary Figs. 1–5). Here, we present the 115 single tree-ring <sup>14</sup>C measurements (Supplementary Data 1) performed to locate the 5259 BC Miyake event in all four wood samples selected from the master Dispilio juniper tree-ring chronology (Fig. 3a). An average year-to-year increase (*sensu* Miyake et al.<sup>19</sup>) of -15.8 ‰ in  $\Delta^{14}\text{C}$  was detected in all wood samples (Fig. 3a and Supplementary Data 1) in the exact same dendrochronologically cross-dated tree-rings corresponding to the relative year 184 of the Dispilio juniper chronology. This increase varies from the lowest of -11.1 ‰  $\Delta^{14}\text{C}$  in wood sample DISP-10070, to -13.1 ‰ in DISP-10206, to -14.8 ‰ in DISP-10063, and to -18.6 ‰ in DISP-10611 (Fig. 3a and Supplementary Data 1).

To compare the <sup>14</sup>C results from Dispilio with the published reference data for the 5259 BC event, a mean-value annually resolved reference curve (RC) was established from the dataset in Brehm et al.

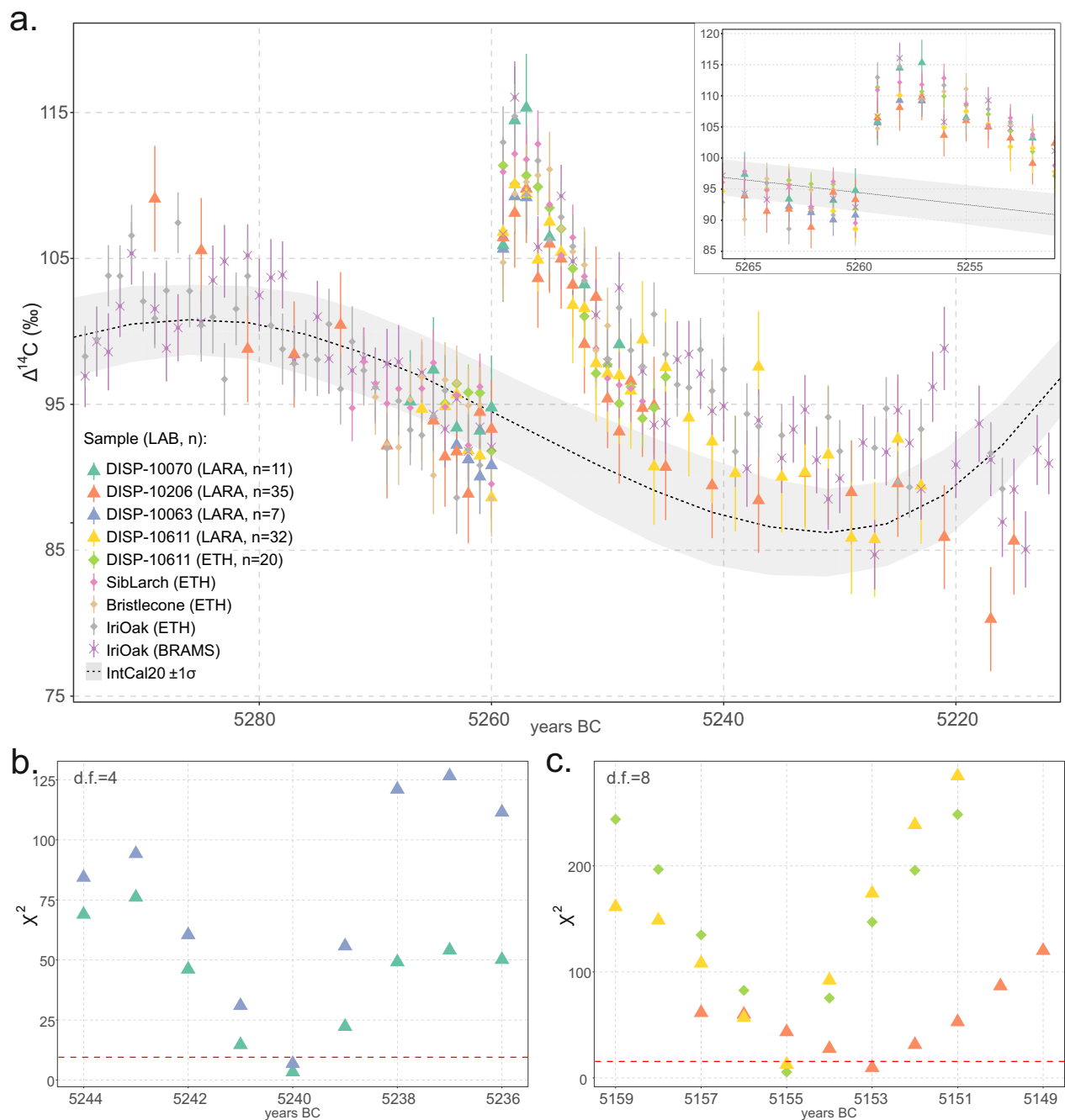


**Fig. 3 |** Scatter plot of  $\Delta^{14}\text{C}$  data from Dispilio against reference from Brehm et al.<sup>22</sup> and IntCal20<sup>70</sup>, and best last ring-fit for the dated wood samples ( $\chi^2$ ).

**a** Measured  $^{14}\text{C}$  concentrations represented as  $\Delta^{14}\text{C}$ , vertical bars represent  $1\sigma$  errors (Supplementary Data 1); legend labels marked with “DISP-” and larger symbols refer to wood samples from Dispilio and corresponding  $^{14}\text{C}$  measurements obtained in this study; other labels represent data from Brehm et al.<sup>22</sup>, measurements from Siberian larch, Bristlecone pine, and Irish oak measured at two different labs, symbol shapes according to Lab; Bristlecone pine  $^{14}\text{C}$  data are shifted forward by 1 year from the original BR22 publication following a correction to the dating of

the bristlecone master tree-ring chronology (Supplementary Note 2); shaded band represents IntCal20<sup>70</sup>. Inset in right corner same as in main panel **a**, but at higher resolution, spanning 14 years centred around the  $^{14}\text{C}$  spike. Lower two panels:  $\chi^2$  tests of Dispilio measurements against the average from BR22<sup>22</sup>, **b**,  $\chi^2$  test results for wood samples DISP-10,070 and DISP-10063 ( $\chi^2$  crit. value = 9.49), and **c** for wood samples DISP-10206 and DISP-10611 ( $\chi^2$  crit. value = 15.51), legend as in panel above. Figure panels produced in R<sup>101</sup>, code and source data available in Supplementary Data 3.

(2022: henceforth referred to as ‘BR22’<sup>22</sup>). A common approach to verifying the position of Miyake events is wiggle-matching using a goodness-of-fit  $\chi^2$  test<sup>9,10,71</sup> against a reference, so that the  $\chi^2$  value becomes minimal for the correct placement of the sample’s wane-edge<sup>68</sup>. The lowest  $\chi^2$  values are reached when the end-dates of the wood samples are placed at 5240 BC for DISP-10070 and DISP-10063 (Fig. 3b), 5153 BC for DISP-10206, and 5155 BC for DISP-10611 (Fig. 3c),

corresponding to their cross-dated position along the tree-ring chronology. The 5259 BC event signal is clearly identified in all wood samples (Fig. 3a).

To test how close conventional radiocarbon wiggle-matching would be relative to the absolute calendar dating supplied by the Miyake event, the annual data from all four wood samples were wiggle-matched against the IntCal20 calibration curve<sup>70</sup> using the

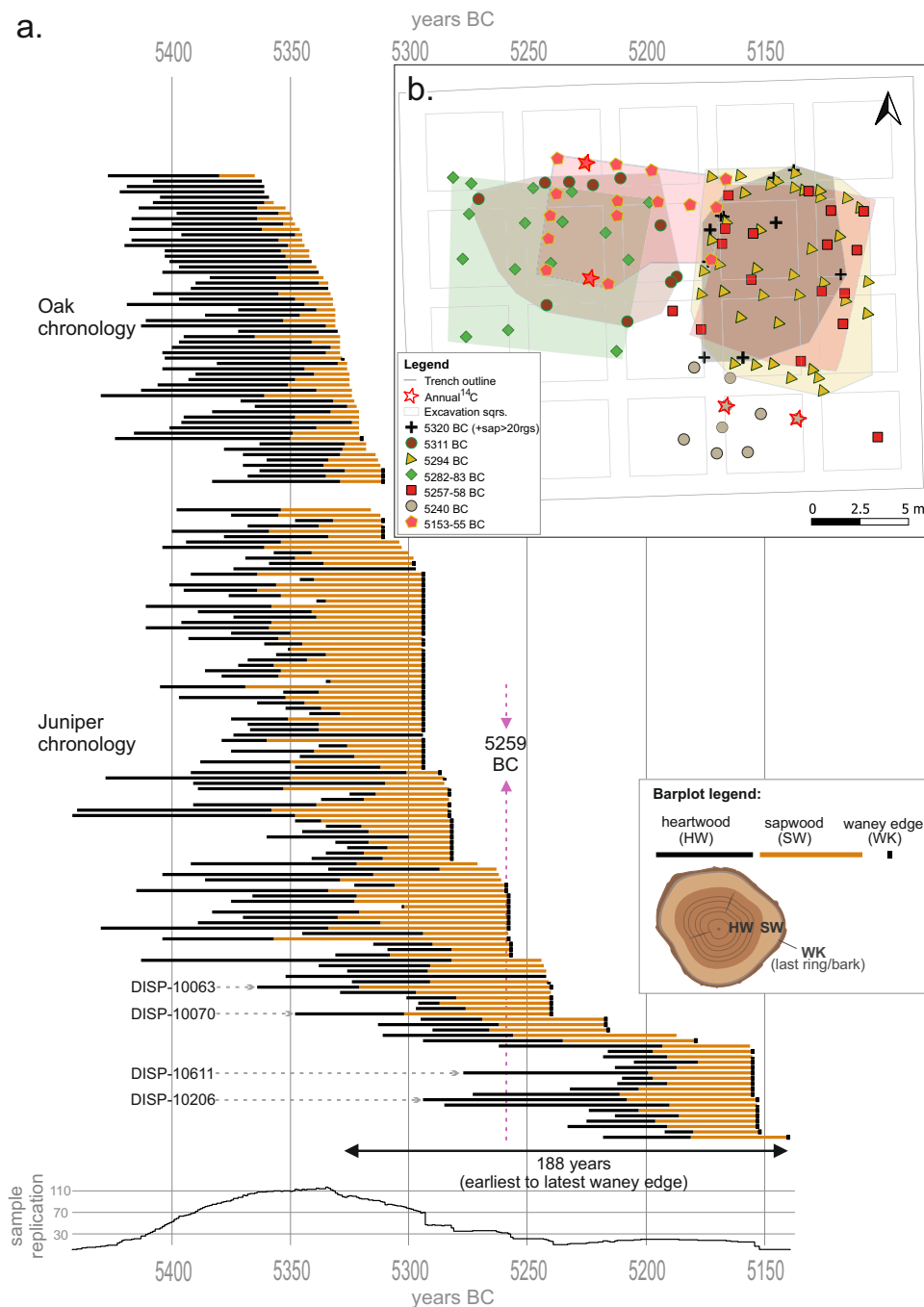


**Fig. 4 | Bar chart of tree-ring chronologies, felling dates, and archaeological site plan development of the East Sector, Dispilio, Greece.** **a** bar plot of Dispilio oak and juniper chronologies, calendar-year dating as obtained by identifying the radiocarbon spike of 5259 BC<sup>22</sup> in the juniper chronology; each horizontal bar represents an individual wood sample in its dendrochronologically cross-dated position; bar length corresponds to its span in years measured by number of tree-rings; bar plot legend with the drawing of a wood sample cross-section schematically describes the meaning of each horizontal bar; “DISP-...” labels and dashed

lines with arrows point to the location in the tree-ring chronology of the wood samples sampled for annual  $^{14}\text{C}$  (Supplementary Figs. 1-5). **b** schematic plan of the East Sector (see also Fig. 1c, d); each symbol represents one vertical wooden element, different shapes and colours correspond to the same felling phase spread over 1–2 years; additionally, the colour-shaded polygons outline the groups of same symbols (same felling-phase wooden piles), however they do not represent definite structure plans; red stars represent the location on the site plan of the wood samples in which the radiocarbon spike of 5259 BC was identified.

OxCal 4.4  $^{14}\text{C}$  calibration software<sup>68,69</sup>. When IntCal20 is used, in none of the cases does the 95% probability end-date range include the actual felling date (Fig. 5 and Supplementary Data 3). Longer series of  $^{14}\text{C}$  dates that span some years before and after the event (Figs. 3a and 5), such as from wood samples DISP-10611 and DISP-10206, yield end-dates that are only -15–20 cal years older, and shorter series, such as from wood samples DISP-10070 and DISP-10063, result in

end-dates over ~40 cal years younger than the actual felling dates (Fig. 5). It has been noted previously<sup>72</sup> that IntCal20 is poorly replicated during the 53<sup>rd</sup> and 52<sup>nd</sup> centuries BC. Notably, the 53<sup>rd</sup> century BC is represented by only 16 measurements, of which 14 are decadal and bi-decadal blocks of 10–20 tree-rings, with only two 4-year and 5-year blocks<sup>70,73</sup>(Supplementary Fig. 8). The variability in the calibrated end-date ranges suggests that IntCal20 might produce

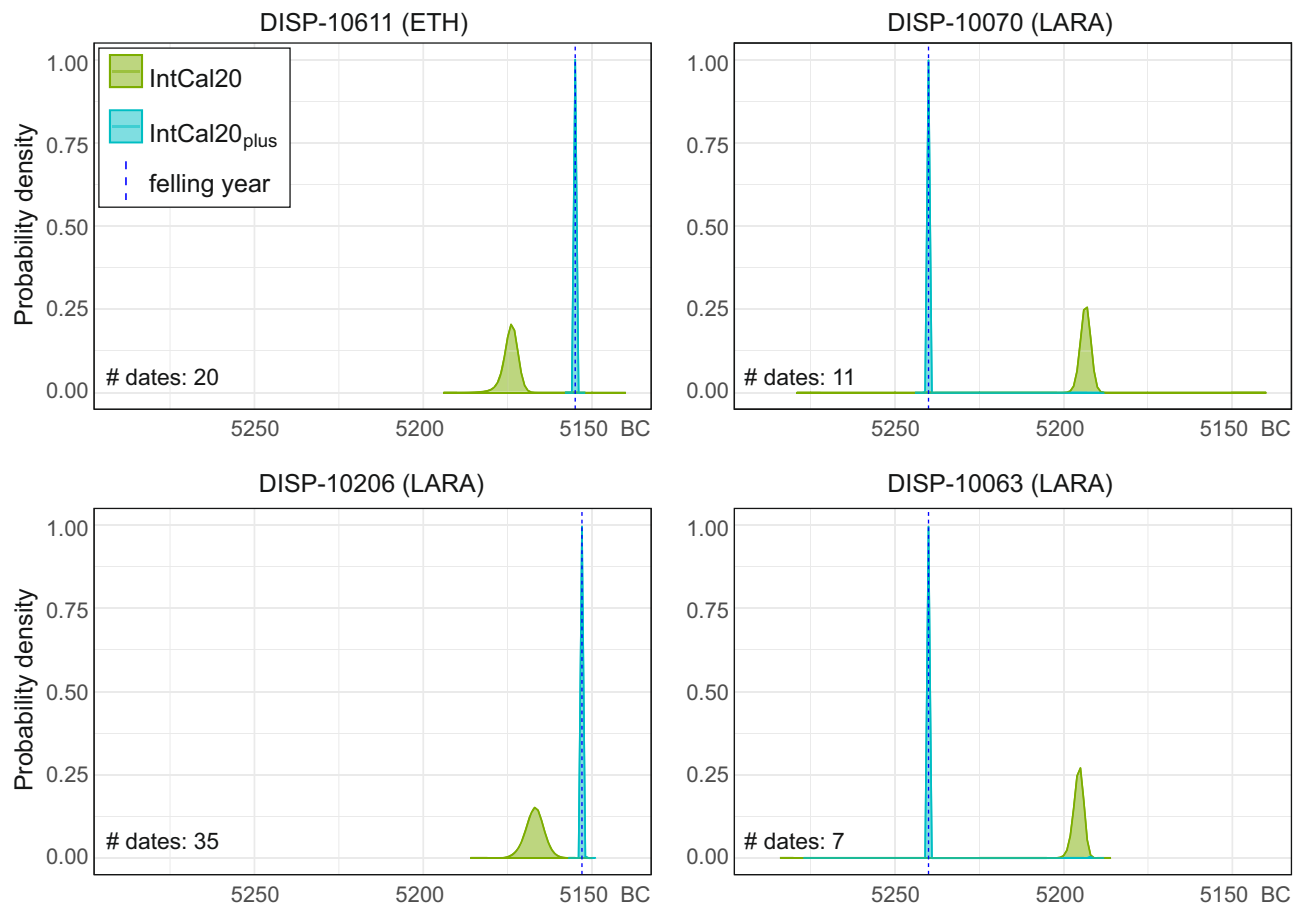


**Fig. 5 | Probability distributions of end-date ranges produced by wiggle-matching different sets of annual  $^{14}\text{C}$  data from Dispilio modelled in OxCal v4.4, against IntCal20<sup>70</sup>, and IntCal20plus.** In IntCal20plus the non-annual IntCal20 data for a 82-year period around the 5259 BC Miyake event is replaced by the annual average of Brehm et al.'s<sup>22</sup> annual data. Dashed blue lines represent

actual felling dates determined through dendrochronology and Miyake event-matching. Acronyms in brackets next to sample name refer to the AMS lab that furnished the measurements. Data for figure obtained from OxCal 4.4<sup>68,69</sup>. Figure produced in R<sup>101</sup>, R code, OxCal code and source data in Supplementary Data 3.

misleading results when wiggle-matching annual data coming from the period in question. The annual  $^{14}\text{C}$  dates were also wiggle-matched against a modified IntCal20, IntCal20plus, in which the default IntCal20 multiple-year blocks of before-present (BP) data for the 82-year period around the event were substituted with the average of the annual BR22 dataset. Calibrating against this dataset predictably yields the accurate and more precise end-date ranges at 95% probability for all wood samples (Fig. 5).

The growing season of trees is influenced by many factors and can vary between and within species as a function of cambial age, temperature, water availability, slope, aspect, soil type, and other factors. Personal observations of growth termination in modern oaks and junipers in the region have shown that latewood width at breast height can be completed in both genera by the beginning of September (Supplementary Figs. 6 and 7). While cell-wall thickening in temperate conifers continues for several weeks after the cessation of cell-wall enlargement<sup>74</sup>, the amount of cellulose carbon that would be deposited during this last stage of latewood formation constitutes a small percentage of the whole tree-ring<sup>75</sup>. Considering the robustness of the  $^{14}\text{C}$  signal in the Dispilio junipers tree-rings (Fig. 3) it is unlikely that it only represents the  $^{14}\text{C}$  incorporated at the end of the cell-wall thickening stage. Consequently, it can be inferred that the  $^{14}\text{C}$  signal of the 5259 BC event in the indeciduate junipers has been incorporated during the temperate growing season between spring and late summer/early autumn 5259 BC.

According to the dendrochronologically cross-dated position of all wood samples, the ring in which the Miyake event is detected corresponds to relative year number 184 of the 303-year-long juniper TRW chronology. This allows us to set the absolute end-date of the whole Dispilio juniper tree-ring chronology at 5140 BC. Furthermore, the identification of the event in wood samples DISP-10070 and DISP-10063 confirms the correct placement of the better-replicated earlier half of the chronology (Fig. 4a). Given the dendrochronological cross-dating between the juniper and oak chronologies, also the latter is absolutely dated, placing its last ring at 5311 BC (Fig. 4a).

### Site plan and felling phases

The timespan of 188 years between the earliest and latest felling dates (Fig. 4a) indicates the minimum duration of construction activities during Dispilio's 54<sup>th</sup>–52<sup>nd</sup> centuries BC settlement phases. This timespan between 5328 and 5140 BC includes intermittent periods of wood felling and construction (Fig. 4a, b). However, the timespan between the earliest and latest felling dates in Dispilio need not alone reflect a continuous, uninterrupted occupation of the same location.

Wooden piles that have been dendrodated against the Dispilio juniper master chronology with felling dates within 1–2 years of one another, were plotted on the site plan using a GIS software (Fig. 4b). This revealed outlines that probably represent different structures (Fig. 4b). Identification of building outlines was possible only for groups that are composed of a substantial number of dendrodated

samples. The structures seem to be oriented along the modern lake-shore; however, the shape of the Neolithic lakeshore is uncertain. Of note is the concentration of building activities in the eastern part of the East Sector (Fig. 4b). In this part, a group of wooden piles with a felling date of 5294 BC outline an area, superimposed by a group of piles with felling dates in 5258–5257 BC (Fig. 4a, b). The juniper group felled in 5294 BC is preceded by a potential felling phase ending in 5320 BC consisting of oak wood samples. However due to the poor preservation of oak sapwood only two of this group have preserved waney edge. These two securely dated piles are complemented by several other oak piles with final measured rings falling between 5328 BC and 5320 BC and no waney edge, but with at least 20 sapwood rings indicating the proximity of the waney edge. The mapping of the dendrochronological results also implies that building practices in some cases included either the short-term storage of timber for 1–2 years or a construction period spread over several years.

## Discussion

No absolute timeframe has been generally agreed for the archaeological periodisation of the Neolithic in the region (e.g. refs. 8,76). Therefore, depending on the sources consulted, the occupation phases of Dispilio discussed here would fall in the later Middle Neolithic and/or Late Neolithic. In this context, the absolute calendar-year dating of Dispilio is a step forward in establishing a more readily navigable periodisation of the Middle and Late Neolithic in the region<sup>8,76</sup>. The precision of the absolute dating and duration of the 54<sup>th</sup>–52<sup>nd</sup> century BC occupation and construction phases in Dispilio is unique not only in the Neolithic of the Balkans, but also in the wider Eastern Mediterranean. The site also provides sufficiently replicated dendrochronological information to serve as an independent control for settlement durations which are mostly estimated from modelled <sup>14</sup>C dates<sup>77,78</sup>.

The felling dates in the excavated sector indicate activity over a period of at least 188 years, and indications from oak sapwood reconstruction estimates may extend this backwards in time by a further ~30 years. Of particular interest is the succession of two construction phases in the western half of the analysed trench and three construction phases in its eastern half (Fig. 4a, b). Although the potential function of these structural outlines (Fig. 4b) is not clear at present, the precise timespans between the construction episodes of 29 years in the western half (5311 and 5282 BC), and 35–37 years in the eastern half (5320, 5294 and 5257 BC) are consistent with the few available estimates of house lifespans in Neolithic S-E Europe<sup>77,78</sup>. However, determining whether these contemporary structure outlines with similar felling dates correspond to one building or more will require further detailed multidisciplinary work. Intermittent periods without felling dates may simply be a result of worse preservation of some elements or the limited size of the excavated area, but they may also reflect a hiatus in occupation, or indicate that settlement was of a nonperennial character. Detection of annual or decadal-scale hiatuses is extremely difficult in archaeological stratigraphy, with settlement phase duration usually estimated from <sup>14</sup>C sequence models based on organic samples from consecutive stratigraphical units. This approach can lead to interpretations of centuries-long settlement continuities<sup>4,79</sup>. Such interpretations may underestimate settlement discontinuities of durations shorter than the precision of <sup>14</sup>C measurements and calibration. This underlines the importance of the annually resolved data from Dispilio.

The last centuries of the 6th millennium BC mark an important change within the Neolithic period in the southern Balkans. It is a period of a steep increase in the number and size of settlements, associated with a demographic boom<sup>8,80–82</sup>. Anthropogenic influence on the local environment becomes pronounced during this period<sup>83,84</sup>, as also documented at Dispilio<sup>43,44</sup>. Diversity increased in all aspects of human behaviour, from pottery production techniques and styles<sup>85</sup>,

architecture<sup>81</sup>, settlement organisation<sup>81,86,87</sup>, to the first signs of metallurgy<sup>88</sup>. Evidence from this period also indicates a shifting social focus from the collective to the domestic<sup>89,90</sup>, when individual households seem to play a more prominent role in community life. In this setting, high-resolution chronological data can improve our understanding of societal changes, human land use, and intensifying influence on the local and regional environment. For instance, the preference for settling in the proximity of wetlands has been documented in the Early Neolithic<sup>3,91</sup>, and the practice continued in the Middle and Late Neolithic<sup>36,91</sup>. Wetland and shoreline locations would have represented ideal catchment areas for the Neolithic subsistence, providing various soil types that could be used for cultivating crops with different requirements, serve as pasture lands, or supply aquatic resources as a dietary complement<sup>91</sup>. A number of wetland sites with similar chronology to Dispilio's phases discussed here (2<sup>nd</sup> half of the 6<sup>th</sup> millennium BC) have been documented or excavated in existing or former lakes in the region (Fig. 1b), some of them yielding large amounts of well-preserved wooden construction elements<sup>36–38,92–94</sup>. Although the dating of these sites has much lower chronological resolution than at Dispilio, some of them would have been in use for centuries before and/or after the 54<sup>th</sup>–52<sup>nd</sup> century BC phases at Dispilio. It is highly likely that it will be possible to cross-date the tree-ring widths of the wood remains from these neighbouring sites with the now absolutely dated tree-ring chronologies from Dispilio, and thus extend the absolutely dated dendrochronological network for the region well beyond the 6th millennium BC.

Beyond the chronological significance, absolutely dated tree-ring records are one of the most frequently used proxies for high-resolution climate reconstructions and offer unique insights into the relationship between societies and climate. Precipitation is a limiting factor for most low and mid-altitudes trees in the Eastern Mediterranean. In fact, modern juniper<sup>53</sup> and oak<sup>17,95</sup> tree-ring sequences have been shown to be good predictors of precipitation in the Eastern Mediterranean. Precipitation was a crucial factor in early agriculture, which mainly consisted of rainfed<sup>96</sup> and floodwater<sup>97</sup> farming. Preliminary observations of the Dispilio TRW chronologies indicate a period of suppressed growth in both the juniper and oak tree-ring sequences for a period of around 20 years between 5360 and 5340 BC. Such a period of suppressed growth can be associated with a decrease in precipitation, which may have influenced the water table of small water bodies such as Lake Kastoria. A short-term Mid/Late Neolithic eutrophication of the lake previously inferred from the increased occurrence of green algae<sup>39</sup> could potentially be correlated with this tree-ring width suppression. Although the Neolithic tree-ring sequences from Dispilio are relatively short if compared to modern tree-ring proxies used in climate reconstructions, they may still provide valuable, absolutely dated, annually resolved information on environmental conditions during the Neolithic in Kastoria Basin and the surrounding region.

Finally, the results from this study underline the value that single-year measurements of radiocarbon in tree-rings can have for radiocarbon calibration and dendrochronological dating. Significant advances in AMS technology<sup>98</sup>, have enabled the creation of continuous time-series of annual radiocarbon measurements that are constantly improving the resolution of the radiocarbon calibration curve, thereby increasing the accuracy of the radiocarbon calibration process. Moreover, the value of SEP events in anchoring regional timelines through hybrid tree-ring and radiocarbon studies is once again demonstrated. The <sup>14</sup>C-anchored Dispilio tree-ring chronologies now provide a calendar-dated reference for dendrochronological dating of other sites from the time period. This provides the opportunity to extend calendar-dated chronologies across the region further back into prehistory. Such high-resolution dating, especially when it can be coupled with stratigraphic information or used to derive climatic indicators, will elucidate a more

nuanced understanding of deterministic interpretations of the environmental influence on societies in the past, for instance for the 6.2 ka BC cooling event. This study demonstrates how the recent discovery of the SEP events in this time period creates new possibilities in prehistoric archaeology and offers the construction of historical-timescale narratives for societies and their environments from the very distant past.

## Methods

### Wood samples

The wood material analysed in this study was sampled in August and September 2019 from wooden piles remains at the archaeological site of Dispilio, near Kastoria, Greece (40.485444 N, 21.289694 E; h = 627 masl). The site is one of the best-known prehistoric sites in the country and has been investigated, almost continuously, since 1992. Excavations and sampling that took place on the site were performed in full compliance with the regulations of the Greek Ministry of Culture concerning archaeological material. The permit number for the wood samples obtained from the Ministry is: ΥΠΠΟΑ/ΓΔΑΠΚ/ΔΣΑΝΜ/ΤΕΕ/Φ77/379195/266411/4122/252, issued on 24.07.2020. During the 2019 fieldwork campaign, whole cross-section discs ( $n = 787$ ) were sampled from the wooden remains with handsaws and chainsaws. The wood samples' documentation, cleaning, preparation, and sealing in plastic bags with water, took place on-site. Dendrochronological measurement began on-site and continued at the University of Bern. Tree-ring width (TRW) measurements were performed according to standard dendrochronological procedures<sup>99,100</sup>, with a measuring table under a binocular stereo microscope. TRWs were recorded with a precision of 0.01 mm. Two to four radii were measured per sample and averaged together to represent the sample. Descriptive dendrochronological statistics were performed in the dplR package in R<sup>59,101,102</sup>. The TRW measurements of DISP-10611, -10206, -10070, and -10063 are available in both Source Data and Supplementary Note 2. All wood specimens will be permanently deposited at the Dispilio Excavation Laboratory, Dispilio, Greece. Access is subject to obtaining permits from the Greek Ministry of Culture.

Wood taxonomy was determined from stem wood anatomy. Each measured wood sample was sectioned with a razor blade and cell arrangements in the transversal, radial, and tangential sections were identified and compared with references in wood-anatomical atlases<sup>55,56,103</sup>. Given the wood-anatomical similarity of various deciduous oak species from the subgenus *Quercus*<sup>56</sup>, and considering the high dendrofloristic diversity of oaks in the region<sup>57,58</sup>, it was not possible to distinguish them to species level. However, several deciduous oak species from the subgenus *Quercus* are likely to be represented, notably *Q. frainetto*, *Q. petraea*, and/or *Q. pubescens*. Oak trees from the subgenus *Cerris* are one of the more abundant groups of oaks in the region; however, no wood samples from Dispilio could be assigned to this group, which is anatomically characterised by larger and solitary latewood pores. Similarly, wood anatomical differentiation between different juniper species was not possible<sup>54,55,103</sup>. Considering today's distribution of tree-like junipers in the region, the species most likely to have been used in Dispilio are *Juniperus excelsa*, *J. foetidissima*, and/or *J. deltoides* Adams (cf. *J. oxycedrus* L.). Although the majority of the pine samples exhibited denticulate walls on end-tracheids, a characteristic of the pine subgenus *Pinus* (cf. *Pinus nigra/sylvestris*-type), several pine wood samples could be identified as members of the subgenus *Strobus* (cf. *P. peuce*) by the presence of smooth-walled end-tracheids.

Modern local climatic conditions in the Kastoria Basin can be defined as continental to sub-Mediterranean, with temperate weather, continental winters, and warm and dry summers. The yearly average precipitation in the lower parts of -700 mm increases with altitude. The wettest months are November and December, and the driest and hottest months are July and August. Yearly average temperature is

-12 °C. Main climate classes according to the Köppen system<sup>104</sup> are Cfa, Cfb, and Csa.

### Sample preparation and radiocarbon measurement

Individual tree-rings were dissected by hand under a binocular microscope with a one-sided razor blade (Supplementary Fig. 5). Whole rings were used for all <sup>14</sup>C measurements (Supplementary Data 1). About 30–70 mg of material was sampled per ring, depending on its width. Earlywood comprises ca. 80–90% of a juniper tree-ring. Because most of the of the ring-width of junipers growing on mesic sites is completed by the end of September<sup>105</sup> (see also Supplementary Figs. 6 and 7), the tree-ring structural carbon concentration should reflect temperate spring-to-late summer carbon uptake.

Wiggle-matching of 11 <sup>14</sup>C dates from the juniper chronology (modelled end-date 5233–5137 cal BC, 95% probability, Supplementary Note 1) provided the basis for an initial estimate of the segment on the tree-ring chronology where the event was to be located. A series of 70 individual tree-rings centred around an estimated event ring were dissected from the first wood sample that was analysed (DISP-10206, Supplementary Fig. 1). The <sup>14</sup>C content of every 4<sup>th</sup> sampled ring was subsequently measured until the <sup>14</sup>C spike was identified, after which the <sup>14</sup>C in 20 consecutive rings around the event was measured (Supplementary Data 1). The event ring on all the other wood samples (DISP-10611, DISP-10070, and DISP-10063, Supplementary Figs. 2–4) was identified according to the samples' dendrodated position along the tree-ring chronology.

Cellulose from wood samples analysed at the Laboratory for the Analysis of Radiocarbon with AMS at the University of Bern (LARA)<sup>106</sup> was extracted following the BABAB method<sup>107</sup> including Sookdeo et al.'s.<sup>98</sup> modifications at 70 °C for all steps. Samples were submerged in a 1 M NaOH overnight and treated in 1 M HCl followed by 1 M NaOH in a shaker for 1 h each. Bleaching of the samples was performed on addition of 5 mL water, a few drops of 1 M HCl to reach pH 2–3 and 100 mg NaClO<sub>2</sub> by shaking for at least 2 h or until the colour of the wood samples turned white. The material was dried by lyophilisation overnight. Samples were measured using the LARA MICADAS AMS system. In June – November 2022 the tree-rings from wood samples DISP-10070, -10206 and a first run of -10611 were analysed together with three oxalic acid II (SRM 4990 C, NIST) standards and three chemical blanks. In June 2023, DISP-10063 and a second run of DISP-10611 were dated together with five oxalic acid II standards and four chemical blanks that were used for blank subtraction, standard normalisation, and correction for isotope fractionations. Two IAEA-C5, two IAEA-C7, two 1515 CE reference samples and two cellulose blanks were also used as secondary standards and blanks, respectively. All initial results (Supplementary Data 1) were biased by an inappropriate batch of the oxalic acid II standard that was used for the measurements. A total of ten samples from our first run of DISP-10611 were repeated within our second run which gained an average negligible difference between both LARA runs of 0.6‰ so that our DISP-10611 dataset that is shown Fig. 3a represents the average of both LARA runs (Supplementary Data 2). By intercomparison with three other oxalic acid II batches (one of which was provided by ETHZ), an offset corresponding to a <sup>14</sup>C age of +30.9 ± 3.2 years was determined for the inappropriate batch, whereas the results of the oxalic acid II of the other three batches were identical within uncertainties. The initial results were corrected for this offset yielding a shift of -4.2‰ for the samples. The corrected results are presented in Fig. 3a.

For the analyses performed at the Laboratory of Ion Beam Physics at ETH Zürich (ETH), the tree-ring samples were prepared in 15 ml glass test tubes together with four wood blanks (2 BC and 2 KB) and 2 1515 CE reference samples each weighing 30–60 mg<sup>98,108</sup>. In a slightly modified procedure following<sup>107</sup>, samples were first soaked in 5 ml 1 M NaOH overnight at 70 °C in an oven. Then the samples were treated with 1 M HCl and 1 M NaOH for 1 h each at 70 °C in a heat block, before they



were bleached at a pH of 2–3 with 0.35 M NaClO<sub>2</sub> at 70 °C for 2 h. The remaining white holo-cellulose was then freeze-dried overnight. ~2.5 mg dried holo-cellulose was wrapped in cleaned Al capsules and converted to graphite using the AGE-3 automated graphitisation line. A measurement set was assembled comprising the tree-ring samples, three oxalic acid one (OX1) and four oxalic acid two (OX2) standards, two cellulose blanks, two chemical blanks, and two 1515 CE reference samples and measured in the MICADAS accelerator mass spectrometer.

### Radiocarbon matching and modelling

The <sup>14</sup>C measurements presented in this study were matched to the constructed reference curve<sup>22</sup> (Supplementary Data 3) using a common  $\chi^2$  test approach (Eq. (1)) so that the  $\chi^2$  value becomes minimal for the correct placement of the sample's wane-edge<sup>9,10,68</sup>:

$$\chi^2(x) = \sum_{i=1}^n \frac{(R_i - C_{(x-r_i)})^2}{\delta R_i^2 + \delta C_{(x-r_i)}^2} \quad (1)$$

here  $R_i \pm \delta R_i$  represent the new <sup>14</sup>C measurements,  $C_{(x-r_i)} \pm \delta C_{(x-r_i)}$  represent the reference curve <sup>14</sup>C concentrations in the year  $(x - r_i)$ ;  $x$  is the assumed calendar year; and  $r_i$  stands for the tree ring number starting with 0, representing the last growth ring of the tree (wane edge).

The Bayesian wiggle-matching was performed in the OxCal 4.4 software with the D\_Sequence command against the atmospheric data from IntCal20<sup>69,70</sup>. For the CQL code see Supplementary Note 1, and the end of the.Rmd file in Supplementary Data 3.

The year-to-year increase in  $\Delta^{14}\text{C}$  presented in the Results section was calculated as a difference between the values in 5260 BC and 5259 BC (*sensu* Miyake et al.<sup>19</sup>). For a detailed discussion on the magnitude and <sup>14</sup>C production during the 5259 BC Miyake event see<sup>22</sup> and<sup>109</sup>.

Calendar years are expressed according to the Gregorian calendar (AD/BC), without year 0.

### Data uncertainty

The genus *Juniperus* is known to produce intra-annual density fluctuation ('false rings'), and to have 'missing rings'<sup>110</sup> in parts of the stem. Missing rings are very often a product of the stem growth habit of junipers, termed 'lobate growth', which involves higher cambial activity and faster growth in certain areas of the stem, resulting in an undulating cross-section of the stem in older trees, where the less active areas may not produce rings in certain years. However, missing rings or measuring false rings can be accounted for when sufficient numbers of wood samples with complete stem cross-sections are available, as in Dispilio. The correct location of the "event ring" on all wood samples determined from their cross-dated position further supports an accurate ring count. Moreover, the dendrochronological cross-dating of the first half of the juniper chronology against the oak chronology provides an additional control for the correct ring count, because oak trees hardly ever have missing rings<sup>111</sup>.

### Reporting summary

Further information on research design is available in the Nature Portfolio Reporting Summary linked to this article.

### Data availability

Supplementary Data 1-2, Supplementary Information including Supplementary Notes 1-2 and Supplementary Figs., as well as Supplementary Data 3 for this paper are available both at the journal's website, and also at the following repository: <https://doi.org/10.5281/zenodo.8407222> [<https://zenodo.org/records/10981405>]. The use of DOI resolver is recommended for being directed to the latest version

of the Supplementary Information. Individual tree-ring width measurements of wood samples not discussed in the text are available on request, as they will form part of an upcoming dedicated publication. Source data are provided with this paper.

### Code availability

OxCal code is available in the Supplementary Information file in the section Supplementary Note 1, and at the bottom of the.rmd file in the Supplementary Data 3.

### References

- Grosman, L. *Natufian Foragers in the Levant: Terminal Pleistocene Social Changes in Western Asia* (eds. Bar-Yosef, O. & Valla, F. R.) 622–637 (Berghahn Books, 2013).
- Maniatis, Y. In *A Century of Research in Prehistoric Macedonia 1912-2012, International Conference Proceedings, Archaeological Museum of Thessaloniki, 22-24 November 2012* (eds. Stefani, E., Merousis, N. & Dimoula, A.) 205–222 (Archaeological Museum of Thessaloniki, 2014).
- Karamitrou-Mentessidi, G., Efstratiou, N., Kaczanowska, M. & Kozłowski, J. Early Neolithic settlement of Mavropigi in western Greek Macedonia. *Eurasia. Prehist.* **12**, 47–115 (2015).
- Maniatis, Y. & Adaktylou, F. Revenia-Korinos: one of the earliest Neolithic settlements in North Greece as evidenced by radiocarbon dating. *Radiocarbon* **63**, 1025–1051 (2021).
- Horejs, B. et al. The Aegean in the Early 7th Millennium BC: Maritime Networks and Colonization. *J. World Prehist.* **28**, 289–330 (2015).
- Starnini, E. The figurines of the Early Neolithic settlement of Mavropigi (Western Greek Macedonia) and their significance in the neolithization process of Greece. *Eurasia. Prehist.* **14**, 55–152 (2018).
- Shennan, S. *The First Farmers of Europe* (Cambridge University Press, 2018).
- Tsirtsoni, Z. Chapter 1. *The Human Face of Radiocarbon* (ed. Tsirtsoni, Z.) 13–39 (MOM Éditions, 2016).
- Wacker, L. et al. Radiocarbon dating to a single year by means of rapid atmospheric <sup>14</sup>C changes. *Radiocarbon* **56**, 573–579 (2014).
- Kuitemans, M. et al. Evidence for European presence in the Americas in AD 1021. *Nature* **601**, 388–391 (2022).
- Meadows, J., Zunde, M., Lēģere, L., Dee, M. W. & Hamann, C. Single-year <sup>14</sup>C dating of the lake-lortress at Āraiši, Latvia. *Radiocarbon* <https://doi.org/10.1017/RDC.2023.24> (2023).
- Philippson, B., Feveile, C., Olsen, J. & Sindbæk, S. M. Single-year radiocarbon dating anchors Viking Age trade cycles in time. *Nature* **601**, 392–396 (2022).
- Schweingruber, F. H. *Tree Rings: Basics and Applications of Dendrochronology* (Kluwer Academic Publishers, 1988).
- Friedrich, M. et al. The 12,460-Year Hohenheim Oak and Pine Tree-Ring Chronology from Central Europe—a unique annual record for radiocarbon calibration and paleoenvironment reconstructions. *Radiocarbon* **46**, 1111–1122 (2004).
- Salzer, M. W. & Hughes, M. K. Bristlecone pine tree rings and volcanic eruptions over the last 5000 yr. *Quat. Res.* **67**, 57–68 (2007).
- Nicolussi, K. et al. A 9111 year long conifer tree-ring chronology for the European Alps: a base for environmental and climatic investigations. *Holocene* **19**, 909–920 (2009).
- Griggs, C., Degaetano, A. & Newton, M. A regional high-frequency reconstruction of May – June precipitation in the north Aegean from oak tree rings, A. D. 1089 – 1989. *Int. J. Climatol.* **27**, 1075–1089 (2007).
- Nicolussi, K., Matuschik, I. & Tegel, W. *Dendro – Chronologie – Typologie – Ökologie. Festschrift für André Billamboz zum 65. Geburtstag* (eds. Bleicher, N., Schlichtherle, H., Gassman, P. & Martinelli, N.) 61–77 (Freiburg im Breisgau : Janus-Verlag, 2013).

19. Miyake, F., Nagaya, K., Masuda, K. & Nakamura, T. A signature of cosmic-ray increase in 774-775 from tree rings in Japan. *Nature* **486**, 240–242 (2012).
20. Miyake, F., Masuda, K. & Nakamura, T. Another rapid event in the carbon-14 content of tree rings. *Nat. Commun.* **4**, 1748 (2013).
21. Dee, M. W. & Pope, B. J. S. Anchoring historical sequences using a new source of astro-chronological tie-points. *Proc. R. Soc. A Math. Phys. Eng. Sci.* **472**, 20160263 (2016).
22. Brehm, N. et al. Tree-rings reveal two strong solar proton events in 7176 and 5259 BCE. *Nat. Commun.* **13**, 1–8 (2022).
23. Pearson, C. et al. Annual Variation in Atmospheric C between 1700 BC and 1480 BC. *Radiocarbon* **62**, 939–952 (2020).
24. Büntgen, U. et al. Tree rings reveal globally coherent signature of cosmogenic radiocarbon events in 774 and 993 CE. *Nat. Commun.* **9**, 3605 (2018).
25. Park, J., Southon, J., Fahrni, S., Creasman, P. P. & Mewaldt, R. Relationship between solar activity and  $\Delta 14C$  peaks in AD 775, AD 994, and 660 BC. *Radiocarbon* **59**, 1147–1156 (2017).
26. Cliver, E. W., Schrijver, C. J., Shibata, K. & Usoskin, I. G. Extreme solar events. *Living Rev. Sol. Phys.* **19**, 2 (2022).
27. Usoskin, I. & Miyake, F. Introduction. In *Extreme Solar Particle Storms - The hostile Sun* (eds. Miyake, F., Usoskin, I. & Poluianov, S.) 1–3 (IOP Publishing, 2019).
28. Uusitalo, J. et al. Solar superstorm of AD 774 recorded subannually by Arctic tree rings. *Nat. Commun.* **9**, 3495 (2018).
29. Mekhaldi, F. et al. Multiradionuclide evidence for the solar origin of the cosmic-ray events of AD 774/5 and 993/4. *Nat. Commun.* **6**, 8611 (2015).
30. Sakurai, H. et al. Prolonged production of  $^{14}C$  during the -660 BCE solar proton event from Japanese tree rings. *Sci. Rep.* **10**, 660 (2020).
31. Tegel, W., Muigg, B., Skiadaresis, G., Vanmoerkerke, J. & Seim, A. Dendroarchaeology in Europe. *Front. Ecol. Evol.* **10**, 1–31 (2022).
32. Mazzucco, N. et al. Multiproxy study of 7500-year-old wooden sickles from the Lakeshore Village of La Marmotta. *Italy Sci. Rep.* **12**, 14976 (2022).
33. Bleicher, N. et al. Middens, currents and shorelines: complex depositional processes of waterlogged prehistoric lakeside settlements based on the example of Zurich-Parkhaus Opéra (Switzerland). *J. Archaeol. Sci.* **97**, 26–41 (2018).
34. Hafner, A. et al. First absolute chronologies of neolithic and bronze age settlements at lake Ohrid based on dendrochronology and radiocarbon dating. *J. Archaeol. Sci. Rep.* **38**, 1–30 (2021).
35. Reich, J. et al. A novel Structure from Motion-based approach to underwater pile field documentation. *J. Archaeol. Sci. Rep.* **39**, 103120 (2021).
36. Chrysostomou, P., Jagoulis, T. & Mäder, A. The ‘Culture of Four Lakes’: Prehistoric lakeside settlements (6th - 2nd mill. BC) In the Amindeon Basin, Western Macedonia, Greece. *Archäol. Schweiz* **38**, 24–32 (2015).
37. Westphal, T., Tegel, W., Heussner, K. U., Lera, P. & Rittershofer, K.-F. Erste dendrochronologische Datierungen historischer Hölzer in Albanien. *Archaeol. Anz.* <https://publications.dainst.org/journals/aa/82/4764> (2010).
38. Naumov, G. Prähistorische Pfahlbauten im Ohrid-See, Republik Mazedonien. *Plattf. Jahrb. des. Ver. für Pfahlbau- und Heimatkd. e. V.* **201**, 10–19 (2016).
39. Karkanas, P. et al. Palaeoenvironments and site formation processes at the Neolithic lakeside settlement of Dispilio, Kastoria, Northern Greece. *Geoarchaeology* **26**, 83–117 (2011).
40. Hourmouziadis, G. *Δισπηλιό. 7500 χρόνια μετά /Dispilio. 7500 years after (in Greek)*. (University Studio Press, 2002).
41. Bolliger, M. et al. Dendroarchaeology at Lake Ohrid: 5th and 2nd millennia BCE tree-ring chronologies from the waterlogged site of Ploča Mičov Grad, North Macedonia. *Dendrochronologia* **79**, 126095 (2023).
42. Maczkowski, A. et al. The Early Bronze Age dendrochronology of Sovjan (Albania): a first tree-ring sequence of the 24th – 22nd c. BC for the southwestern Balkans. *Dendrochronologia* **66**, 125811 (2021).
43. Kouli, K. & Dermitzakis, M. D. 11. Lake Orestíás (Kastoria, Northern Greece). *Grana* **49**, 154–156 (2010).
44. Kouli, K. Plant landscape and land use at the Neolithic lake settlement of Dispilio (Macedonia, Northern Greece). *Plant Biosyst. - Int. J. Deal. all Asp. Plant Biol.* **149**, 195–204 (2015).
45. Ntinou, M. *La paleovegetación en el norte de Grecia desde el Tardiglacial hasta el Atlántico: formaciones vegetales, recursos y usos* (BAR Publishing, 2002).
46. Ntinou, M. Παλαιοπεριβάλλον και ανθρώπινες δραστηριότητες: Η ανθρακολογία στο λιμναίο Νεολιθικό οικισμό στο Δισπηλιό Καστοριάς / Palaeoenvironment and human activities: Wood charcoal analysis at the neolithic lake-settlement at Dispilio, Kastoria (in Greek). *Anaskamma* **04**, 45–60 (2010).
47. Chatzitoulousis, S. Η τεχνολογία του ξυλού στο νεολιθικό λιμναίο οικισμό του Δισπηλιού Καστορίας / Woodworking technology at the Neolithic lakeside settlement of Dispilio, Kastoria (in Greek, English summary). *Anaskamma* **10**, 93–123 (2009).
48. Sofronidou, M. & Dimitriadis, S. Continuity and discontinuity in the pottery of the early phases of neolithic Dispilio (In Greek, English summary). In *A Century of Research in Prehistoric Macedonia 1912-2012, International Conference Proceedings, Archaeological Museum of Thessaloniki, 22-24 November 2012* (eds. Stefani, E., Merousis, N. & Dimoula, A.) 537–548 (Archaeological Museum of Thessaloniki, 2014).
49. Voulgari, E. *Bodies of Clay* (eds. Schwarzberg, H. & Becker, V.) 23–43 (Oxbow Books, 2017).
50. Facorellis, Y., Sofronidou, M. & Hourmouziadis, G. Radiocarbon dating of the neolithic lakeside settlement of dispilio, Kastoria, Northern Greece. *Radiocarbon* **56**, 511–528 (2014).
51. Maczkowski, A., Bolliger, M. & Francuz, J. *Prehistoric Wetland Sites of Southern Europe: Archaeology, Dendrochronology, Palaeoecology and Bioarchaeology*. (eds. Ballmer, A., Hafner, A. & Willy, T.) (Cham: Springer (in press), 2024).
52. Pearson, C. et al. Securing timelines in the ancient Mediterranean using multiproxy annual tree-ring data. *Proc. Natl. Acad. Sci. USA* <https://doi.org/10.1073/pnas.1917445117> (2020).
53. Touchan, R., Akkemik, Ü., Hughes, M. K. & Erkan, N. May–June precipitation reconstruction of southwestern Anatolia, Turkey during the last 900 years from tree rings. *Quat. Res.* **68**, 196–202 (2007).
54. Schweingruber, F. H. *Trees And Wood In Dendrochronology: Morphological, Anatomical, And Tree-ring Analytical Characteristics Of Trees Frequently Used In Dendrochronology* (Springer-Verlag, 1993).
55. Akkemik, Ü. & Yaman, B. *Wood Anatomy of Eastern Mediterranean Species* (Kessel Publishing House, 2012).
56. Schweingruber, F. H. *Mikroskopische Holzanatomie. Formenspektren mitteleuropäischer Stamm- und Zweighölzer zur Bestimmung von rezentem und subfossilem Material. Anatomie microscopique du bois. Microscopic wood anatomy* (Eidgenössische Forschungsanstalt für Wald, Schnee und Landschaft, 1990).
57. Matevski, V. et al. *Forest vegetation of the Galičica mountain range in Macedonia = Шумската вегетација на планината Галичица во Македонија = Gozdna vegetacija gorovja Galičica v Makedoniji* (Biološki institut Jovana Hadžija ZRC SAZU; Makedonska akademija na naukite i umetnostite, 2011).
58. Dida, M. *State of Forest Tree Genetic Resources in Albania, Working Paper FGR/62E*. <http://www.fao.org/3/j2108e/j2108e00.htm#TopOfPage> (2003).

59. Bunn, A. et al. dplR: Dendrochronology Program Library in R; version 1.7.1. <https://CRAN.R-project.org/package=dplR> (2020).
60. Adamopoulos, S. & Koch, G. Wood structure and topochemistry of *Juniperus Excelsa*. *IAWA J.* **32**, 67–76 (2011).
61. Hänninen, T. et al. Ultrastructural evaluation of compression wood-like properties of common juniper (*Juniperus communis* L.). *Holzforschung* **66**, 389–395 (2012).
62. Kuniholm, P. I., Newton, M. W. & Liebhart, R. F. *The New Chronology of Iron Age Gordion* (eds. Rose, C. B. & Darbyshire, G.) 79–122 (University of Pennsylvania Press, 2011).
63. Manning, S. W. et al. Integrated tree-ring-radiocarbon high-resolution timeframe to resolve earlier second millennium BCE Mesopotamian chronology. *PLoS ONE* **11**, 1–27 (2016).
64. Abdrabou, A., Zidan, E., Nishisaka, A., Kurokochi, H. & Yoshimura, S. King Khufu's second boat: scientific identification of wood species for Deckhouse, Canopy, and Forecastle. *Forests* **13**, 2118 (2022).
65. Hollstein, E. *Mitteleuropäische Eichenchronologie: Trierer dendrochronologische Forschungen zur Archäologie und Kunstgeschichte*. (Mainz am Rhein: von Zabern, 1980).
66. Baillie, M. & Pilcher, J. A Simple Crossdating Program for Tree-Ring Research. *Tree-ring Bull.* **33**, 7–14 (1973).
67. Eckstein, D. & Bauch, J. Beitrag zur Rationalisierung eines dendrochronologischen Verfahrens und zur Analyse seiner Aussagesicherheit. *Forstwiss. Cent.* **88**, 230–250 (1969).
68. Bronk Ramsey, C., van der Plicht, J. & Weninger, B. 'Wiggle Matching' Radiocarbon Dates. *Radiocarbon* **43**, 381–389 (2001).
69. Bronk Ramsey, C. Bayesian analysis of radiocarbon dates. *Radiocarbon* **51**, 337–360 (2009).
70. Reimer, P. J. et al. The IntCal20 Northern Hemisphere radiocarbon age calibration curve (0–55 cal kBP). *Radiocarbon* **62**, 725–757 (2020).
71. Kuitens, M. et al. Radiocarbon-based approach capable of sub-annual precision resolves the origins of the site of Por-Bajin. *Proc. Natl. Acad. Sci.* **117**, 14038–14041 (2020).
72. Bayliss, A. et al. IntCal20 Tree Rings: An Archaeological Swot Analysis. *Radiocarbon*. **62**, 1045–1078 (2020).
73. Blaauw, M. *IntCal: Radiocarbon Calibration Curves. R package version 0.3.1*. <https://CRAN.R-project.org/package=IntCal> (2022).
74. Rathgeber, C. B. K., Cuny, H. E. & Fonti, P. Biological basis of tree-ring formation: a crash course. *Front. Plant Sci.* **7**, 1–7 (2016).
75. Cuny, H. E. & Rathgeber, C. B. K. Xylogenesis: coniferous trees of temperate forests are listening to the climate tale during the growing season but only remember the last words! *Plant Physiol.* **171**, 306–317 (2016).
76. Reingruber, A. Timelines in the Neolithic of Southwestern Anatolia, the Circum-Aegean, the Balkans and the Middle Danube Area. In *Making spaces into places: the north Aegean, the Balkans and western Anatolia in the Neolithic* (eds. Tasić, N. N., Urem-Kotsou, D. & Burić, M.) 17–27 (2020).
77. Tasić, N. et al. Interwoven strands for refining the chronology of the neolithic tell of Vinča-Belo Brdo, Serbia. *Radiocarbon* **58**, 795–831 (2016).
78. Bayliss, A. & Whittle, A. *Time and History in Prehistory* (eds. Souvatzi, S., Baysal, A. & Baysal, E.) 123–146 (Routledge, 2018).
79. Stratouli, G. et al. New excavations in Northwestern Greece: the neolithic settlement of avgi. *Kastor. J. Greek Archaeol.* **5**, 63–134 (2020).
80. Weiberg, E. et al. Long-term trends of land use and demography in Greece: a comparative study. *Holocene* **29**, 742–760 (2019).
81. Kotsos, S. *Making spaces into places: the north Aegean, the Balkans and western Anatolia in the Neolithic* (eds. Tasić, N. N., Urem-Kotsou, D. & Burić, M.) 105–123 (Oxford : BAR Publishing, 2020).
82. Elezi, G. *Sociocultural Dimensions Of Production, Use, And Circulation Of Late Neolithic Pottery From Southern Balkans*. (University of California, PhD Thesis, 2020).
83. Lespez, L. et al. The lowest levels at Dikili Tash, Northern Greece: A missing link in the Early Neolithic of Europe. *Antiquity* **87**, 30–45 (2013).
84. Gassner, S. et al. 20,000 years of interactions between climate, vegetation and land use in Northern Greece. *Veg. Hist. Archaeobot.* **29**, 75–90 (2020).
85. Bonga, L. *Late Neolithic Pottery From Mainland Greece, ca. 5,300–4,300 B.C.* (Temple University, 2013).
86. Halstead, P. Farming, material culture, and ideology: repackaging the Neolithic of Greece (and Europe). *Dyn. Neolit. Eur. Stud. honour Andrew Sherratt* 131–151 (2011).
87. Kotsakis, K. What Tells Can Tell: Social Space and Settlement in the Greek Neolithic. In *Neolithic Society in Greece* (ed. Halstead, P.) 66–76 (Sheffield : Academic Press, 1999).
88. Malamidou, D., Tsirtsoni, Z. & Vaxevanopoulos, M. The emergence of metal use in Greek Eastern Macedonia during the Neolithic period (late 6th-5th millennia BC). *Doc. Praehist.* **49**, 2–21 (2022).
89. Kotsakis, K. Domesticating the periphery. New research into the Neolithic of Greece. *Pharos* **20**, 41–73 (2014).
90. Pappa, M. et al. *Diet, Economy and Society in the Ancient Greek World - Towards a Better Integration of Archaeology and Science. Proceedings of the International Conference held at the Netherlands Institute at Athens on 22-24 March 2010* (eds. Voutsaki, S. & Valamoti, S. M.) 77–88 (Peeters, 2013).
91. Gkouma, M. & Karkanas, P. The physical environment in Northern Greece at the advent of the Neolithic. *Quat. Int.* **496**, 14–23 (2018).
92. Giagkoulis, T. *Settling Waterscapes in Europe. The Archaeology of Neolithic and Bronze Age Pile-Dwellings* (eds. Hafner, A., Dolbunova, E., Mazurkevich, A., Pranckenaite, E. & Hinz, M.) 137–155 (Propylaeum, 2020).
93. Korkuti, M. *Neolithikum und Chalkolithikum in Albanien = Néolithique et chalcolithique en Albanie* (Phillip von Zabern Verlag, 1995).
94. Gori, M. *Along the Rivers and Through the Mountains: A revised chrono-cultural framework for the south-western Balkans during the late 3rd and early 2nd millennium BCE. Universitätsforschungen Zur Prähistorischen Archäologie, Band 268*. (Dr. Rudolf Habelt GmbH, 2015).
95. Hughes, M. K. et al. Aegean tree-ring signature years explained. *Tree-Ring Res.* **57**, 67–73 (2001).
96. Halstead, P. & Isaakidou, V. *Farmers at the Frontier* (eds. Gron, K. J., Sørensen, L. & Rowley-Conwy, P.) 77–100 (Oxbow Books, 2020).
97. Van Andel, T. H. & Runnels, C. N. The earliest farmers in Europe. *Antiquity* **69**, 481–500 (1995).
98. Sookdeo, A. et al. Quality dating: a well-defined protocol implemented at ETH for high-precision 14c-dates tested on late Glacial Wood. *Radiocarbon* **62**, 891–899 (2020).
99. Speer, J. H. *Fundamentals of Tree Ring Research* (University of Arizona Press, 2010).
100. Baillie, M. *A Slice Through Time. Dendrochronology and Precision Dating* (Routledge, 1995).
101. R Core Team. R: A Language and Environment for Statistical Computing. <https://www.r-project.org/> (2020).
102. Bunn, A. G. A dendrochronology program library in R (dplR). *Dendrochronologia* **26**, 115–124 (2008).
103. Crivellaro, A. & Schweingruber, F. H. *Atlas of Wood, Bark and Pith Anatomy of Eastern Mediterranean Trees and Shrubs: with a Special Focus on Cyprus*. (Springer-Verlag Berlin Heidelberg, 2013).
104. Beck, H. E. et al. Present and future Köppen-Geiger climate classification maps at 1-km resolution. *Sci. Data* **5**, 180214 (2018).
105. Camarero, J. J., Olano, J. M. & Perras, A. Plastic bimodal xylogenesis in conifers from continental Mediterranean climates. *N. Phytol.* **185**, 471–480 (2010).

106. Szidat, S. et al. 14 C analysis and sample preparation at the new bern laboratory for the analysis of f Radiocarbon with AMS (LARA). *Radiocarbon* **56**, 561–566 (2014).
107. Nēmec, M., Wacker, L., Hajdas, I. & Gāggeler, H. Alternative methods for cellulose preparation for AMS measurement. *Radiocarbon* **52**, 1358–1370 (2010).
108. Wacker, L., Bollhalder, S., Sookdeo, A. & Synal, H.-A. Re-evaluation of the New Oxalic Acid standard with AMS. *Nucl. Instrum. Methods Phys. Res. Sect. B Beam Interact. Mater. At.* **455**, 178–180 (2019).
109. Zhang, Q. et al. Modelling cosmic radiation events in the tree-ring radiocarbon record. *Proc. R. Soc. A.* **478**, 20220497 (2022).
110. Esper, J. Long-term tree-ring variations in Juniperus at the upper timber-line in the Karakorum (Pakistan). *Holocene* **10**, 253–260 (2000).
111. Haneca, K., Āufar, K. & Beeckman, H. Oaks, tree-rings and wooden cultural heritage: a review of the main characteristics and applications of oak dendrochronology in Europe. *J. Archaeol. Sci.* **36**, 1–11 (2009).
112. JPL, N. NASA Shuttle Radar Topography Mission Global 1 arc second [Data set]. Accessed: [https://www.worldclim.org/data/worldclim21.html#google\\_vignette](https://www.worldclim.org/data/worldclim21.html#google_vignette). NASA EOSDIS L. Process. *Distrib. Act. Arch. Cent.* <https://doi.org/10.5067/MEaSURES/SRTM/SRTMGL1.003> (2013).
113. Fouache, E. et al. Palaeogeographical reconstructions of Lake Maliq (Korça Basin, Albania) between 14,000 BP and 2000 BP. *J. Archaeol. Sci.* **37**, 525–535 (2010).
- and wood-anatomical analyses. A.M. sampled individual tree-rings. S.S. and L.W. performed and provided the 14C measurements. A.M., together with C.P., drafted the manuscript, and all authors edited and contributed to the manuscript. A.H. and K.K. obtained funding.

### Competing interests

The authors declare that they have no known competing financial interests or personal relationships that could have appeared to influence the work reported in this paper.

### Additional information

**Supplementary information** The online version contains supplementary material available at <https://doi.org/10.1038/s41467-024-48402-1>.

**Correspondence** and requests for materials should be addressed to Andrej Maczkowski.

**Peer review information** *Nature Communications* thanks Paolo Biagi, Arturo Pacheco-Solana and the other, anonymous, reviewer(s) for their contribution to the peer review of this work. A peer review file is available.

**Reprints and permissions information** is available at <http://www.nature.com/reprints>

**Publisher's note** Springer Nature remains neutral with regard to jurisdictional claims in published maps and institutional affiliations.

**Open Access** This article is licensed under a Creative Commons Attribution 4.0 International License, which permits use, sharing, adaptation, distribution and reproduction in any medium or format, as long as you give appropriate credit to the original author(s) and the source, provide a link to the Creative Commons licence, and indicate if changes were made. The images or other third party material in this article are included in the article's Creative Commons licence, unless indicated otherwise in a credit line to the material. If material is not included in the article's Creative Commons licence and your intended use is not permitted by statutory regulation or exceeds the permitted use, you will need to obtain permission directly from the copyright holder. To view a copy of this licence, visit <http://creativecommons.org/licenses/by/4.0/>.

© The Author(s) 2024

### Acknowledgements

The 2019 fieldwork and the subsequent dendrochronological and radiocarbon analyses were conducted in the framework of the 'Exploring the dynamics and causes of prehistoric land use change in the cradle of European farming' (EXPLO) ERC project. This project is financially supported by the European Union's Horizon 2020 research and innovation programme, under the grant agreement No 810586 (project EXPLO, [exploproject.org](http://exploproject.org)). We would like to thank all the archaeology students involved in the fieldwork and sample curation from the Universities of Thessaloniki and Bern, and the staff of the Ephorate of Antiquities of Kastoria. Thanks are due to Ariane Ballmer for arranging the logistics of the wood sample transport.

### Author contributions

A.M., together with C.P. and A.H., conceived and designed the study. K.K. and T.G. led the fieldwork, and A.M. and J.F. participated in part of it. J.F. and A.M., together with M.B., performed the dendrochronological